Published in final edited form as:
Acad Radiol. 2010 April ; 17(4): 456–463. doi:10.1016/j.acra.2009.12.004.

The Role of Parallel Diffusion-Weighted Imaging and Apparent Diffusion Coefficient (ADC) Map Values for Evaluating Breast Lesions: Preliminary Results

Guangwei Jin[a,b], **Ningyu An**[c], **Michael A. Jacobs**[d], and **Kuncheng Li**[a,*]

[a]Department of Radiology, Xuanwu Hospital, Capital Medical University, Beijing, China 100053

[b]Department of Radiology, MeitanGeneral Hospital, Beijing, China 100028

[c]Department of Radiology,PLA General Hospital, Beijing

[d]The Russell H. Morgan Department of Radiology and Radiological Science and Sidney Kimmel Comprehensive Cancer Center The Johns Hopkins University School of Medicine, Baltimore, MD

Abstract

OBJECTIVE—To evaluate the feasibility of using diffusion-weighted imaging (DWI) with an array spatial sensitivity encoding technique (ASSET) and apparent diffusion coefficient (ADC) map values with different b values to distinguish benign and malignant breast lesions.

MATERIALS AND METHODS—Fifty-six female patients with 60 histologically proven breast lesions and 20 healthy volunteers underwent MRI. A subset of normal volunteers (n = 7) and patients (n = 16) underwent both conventional DWI and ASSET-DWI, and the image quality between the two methods was compared. Finally, ASSET-DWI with b = 0, 600 s/mm^2 and b = 0, 1000 s/mm^2 were compared for their ability to distinguish benign and malignant breast lesions.

RESULTS—The ASSET-DWI method had less distortion, fewer artifacts, and a lower acquisition time than other methods. No significant difference ($P > 0.05$) was detected in ADC map values between ASSET-DWI and conventional DWI. For ASSET-DWI, the sensitivity of ADC values for malignant lesions with a threshold of less than 1.44×10^{-3} mm^2/s (b = 600 s/mm^2) and 1.18×10^{-3} mm^2/s (b = 1000s/mm^2) was 80% and 77.5% respectively. The specificity of both groups was 95%.

CONCLUSION—ASSET-DWI evaluation of breast tissue offers decreased distortion, susceptibility to artifacts, and acquisition time relative to other methods. The use of ASSET-DWI is feasible with b values ranging from 600 to 1000 s/mm^2 and provides increased specificity compared to other techniques. Thus, the ADC value of a breast lesion can be used to further characterize malignant lesions from benign ones.

Keywords

Diffusion-weighted imaging (DWI); MRI; Breast carcinoma; Apparent Diffusion Coefficient (ADC) map

*Address corresponding to likuncheng1955@yahoo.com.cn.

Introduction

Magnetic resonance imaging (MRI) is becoming an essential tool for examination of breast cancer tissue; compared to ultrasound and mammography, it has remarkably high sensitivity due to the use of contrast enhancement material (1–3). Recent multi-center trials have established that dynamic gadolinium contrast enhanced magnetic resonance imaging (DCE-MR) has high sensitivity (>90%) and moderate specificity (~85%) (4,5). Some benign lesions exhibit contrast characteristics that are similar to those of malignant lesions (e.g., fibroadenomas) (6). Therefore, increasing the specificity is a challenge for breast MRI and other imaging methods.

Diffusion-weighted imaging (DWI) is a specific type of MRI. Diffusion is a physical phenomenon that differs from conventional parameters, such as T1 and T2. The principle that underlies diffusion-weighted imaging (DWI) is that the thermal motion of the water molecules in the extracellular fluid enables the acquisition of an image that reflects both histological structure and cellularity. DWI is sensitive to changes in the micro-diffusion of water within the intra- and intercellular environments (7). After an event that has caused a disruption or restriction of the flow of water within a tissue, such as ischemic events (e.g., stroke) or tumor growth, cytotoxic edema occurs and results in changes in the diffusion of water within the tissue (8,9). These changes in the diffusion of water result in changes in the signal intensity on the DWI (either hyperintensity or hypointensity) (8,9). DWI also provides a quantitative biophysical parameter called the apparent diffusion coefficient of water (ADC) map. The ADC map is an indicator of the movement of water within the tissue. It gives an average value of the flow and the distance that a water molecule has moved, and it has been related to the state of tissue during the evolution of cerebral ischemia (10) and tumor progression (11).

Until now, few reports have been published about using the DWI technique to detect and characterize breast tumors (12–17). Some authors have reported lower ADC values for breast cancer tissue compared with normal breast tissue, thus the ADC value may potentially help in differentiating benign and malignant breast tumors (12–17). However, the specificity of the technique is ambiguous. Moreover, traditional echo planar imaging (EPI) DWI can result in distortion of the image by eddy currents and ghosting during the acquisition of the data. Thus, improving DWI quality is another challenge for breast MRI. Resent advancements in hardware, such as phase arrayed coils, have allowed the application newer advanced parallel imaging methods using DWI in evaluating breast tissue. Kuroki et al. (18) used sensitivity encoding SENSE-DWI to decrease ghosting artifacts by acquiring fewer phase encoding steps. In this study, we established the technical feasibility of using echo-planar DWI combined with the array spatial sensitivity encoding technique (ASSET) to evaluate the diagnostic value of ADC in characterizing breast lesions; we also derived a potential diagnostic threshold.

Materials and Methods

This was a retrospective study, and the Ethics Committee of our institution approved the study protocol. All subjects gave written informed consent before beginning the study.

Clinical subjects

Fifty-six women (age range 18–80 years old) with palpable, mammographic or ultrasound-detected breast lesions examined in our hospital were eligible for participation in this study and underwent bilateral MRI examination of the breast between May 2005 to May 2006. None of the patients had been treated in the affected breast within 6 months prior to the

study. Additional exclusions included a prior history of breast cancer in the affected breast, pregnancy, and contraindication to MRI scanning. 20 healthy volunteers (age range 18–66 years old) from the medical examination center of our hospital were included as the control subjects. The criteria for healthy volunteers were no palpable lumps, and no history of breast cancer in the family. In addition, they were not menstruating at the time of imaging.

Clinical and histological analysis

Sixty lesions in the breasts of 56 patients were studied. Fifty-two lesions were confirmed from the surgically excised specimens, which were excised via modified radical mastectomy or lumpectomy, and eight lesions were confirmed from core needle biopsy. Of the 60 lesions, 40 were malignant (39 patients, age range 29–80 years old), including 33 invasive ductal carcinoma, two ductal carcinoma in-situ (DCIS), two mucinous adenocarcinoma, one mucinous adenocarcinoma accompanied with ductal carcinoma, one invasive lobule carcinoma, and one malignant lymphoma. The largest diameter range of the malignant lesions was from 1.3-cm to 6.3-cm (18 lesions≦2-cm; 22 lesions>2-cm).

The 20 benign lesions (17 patients, age range 18– 59 years old) included 10 fibroadenosis, four fibroadenoma, three fibroadenosis accompanied with fibroadenoma, two multiple intraductal papilloma, and one ductal ectasia. The largest diameter range of the benign lesions was from 0.6-cm to 6.1-cm (3 lesions>1-cm; 5 lesions from 1-cm to 2-cm; 12 lesions>2-cm).

MRI protocol

MRI was performed using a dedicated 4-channel phased-array breast coil at 1.5T (GE Excite HD, GE Medical Systems). All subjects were placed in the prone position and underwent the MRI protocol, which included T_1-weighted (T1WI), Saturation Inversion Recovery (STIR) T_2-weighted (T2WI), ASSET-DWI, and dynamic contrast-enhanced T1WI images (DCE-MR). To compare the image quality between the conventional DWI single-shot EPI with ASSET-DWI, a subset of normal volunteers (n = 7) and patients (n = 16) from the original study were randomly chosen to undergo both conventional DWI and ASSET-DWI (b value = 0 and 1000 s/mm^2) to compare image artifacts. The remaining 53 subjects underwent ASSET-DWI only. The sequence parameters were as follows:

- Axial spin echo (SE) T1 weighted images: TR/TE = 600/11.5 ms, 32 slices with a field of view (FOV) of 320~360 mm, 4-mm slice thickness (ST), 1.0 mm interslice gap, 320 × 220 acquisition matrix, 1 NEX (averages)
- Axial T2WI-STIR: TR/TE = 4100/60 ms, 32 slices with a FOV of 320~360-mm, 4 mm ST, 1.0 mm interslice gap, 256 × 512 matrix, 1 NEX
- Axial ASSET-DWI: TR/TE = 6950/58.7 ms, 32 slices with a FOV of 320~360-cm, 4 mm ST, 1.0 mm gap, acquisition matrix of 128 × 128, 2 NEX, ASSET R = 2, b = 0, 600 s/mm^2 and 0, 0100 s/mm^2
- Conventional DWI with EPI: TR/TE = 7750~8000/66 ms, 32 slices with a FOV of 320~360 mm, 4 mm ST, 1.0 mm interslice gap, acquisition matrix of 128 × 128, 2NEX, b = 0, 0, 1000 s/mm^2.
- Pre- and post-contrast axial T1-weighted imaging with Volume Imaging for Breast AssessmeNT (VIBRANT), which comprised 8~10 phases of repeat acquisition before and after a rapid bolus injection of 0.1 mmol/kg body weight of Gd-DTPA (Magnevist, Schering, Berlin, Germany): TR/TE = 5.1/2.5 ms, TI = 17 ms, 2.6 mm ST, matrix of 420 × 310, 0.75 NEX. Acquisition time of every phase was about 57 seconds.

MRI data analysis

The MRI data were analyzed using vendor supplied software (Functool 2, GE Medical Systems) by two radiologists with more than 15 years experience and board certification in body MRI. They were blind to the pathologic results.

Measurement of ADC values—Trace ADC maps were constructed from the DWI images with different gradient factors (b values of 0 and 600 s/mm^2 or b values of 0 and 1000 s/mm^2). The ADC distribution was illustrated on an axial ADC map created with advantage workstation ver.4.2 (GE). The ADC values of the breast lesions of the patients and the breast tissues of the healthy volunteers were automatically measured by drawing the ROI on the DWI images. The size of the ROI in the lesions was smaller than the lesion size, excluding the normal tissue area, in the area of the normal breast tissue was 10 mm in diameter. Each ROI was positioned three times with a change in location, and the radiologists averaged these values.

Measurement of the signal-to-noise ratio (SNR) of the normal breast tissue and the contrast-to-noise ratio (CNR) of the breast lesions—To compare the SNR of the normal breast tissue of healthy volunteers obtained by conventional DWI and ASSET-DWI, we drew the ROI in both the normal breast tissue and in the background tissue behind the breast three times with a change in location to obtain the signal intensity of the normal breast tissue and the standard deviation of the noise. The averages then were calculated. The ROI was placed in the same area of the same slice on conventional DWI and ASSET-DWI. The size of the ROI was 10 mm in diameter. As a reference, we used the fibroglandular tissue that appeared as a homogeneous signal intensity on both the DWI and the T1-weighted images.

The equation used to calculate the SNR of the normal breast tissue is as follows:

$$SNR_n = S_n / SD_b$$

where SNR_n is the SNR of the normal breast tissue, S_n is the signal intensity of normal breast tissue, and SD_b is the standard deviation of the noise in the background.

To compare the CNR of the breast lesion tissues of patients obtained by conventional DWI and ASSET-DWI, we drew the ROI in the lesions, the normal breast tissue, and the background tissue behind the breast three times with a change of the location to obtain the signal intensity of the lesions and normal breast tissue and the standard deviation of the noise. The averages then were calculated. The size of the ROI in the lesions was smaller than the lesion size excluding the normal tissue, and in the area of the normal breast tissue, in the background was 10mm in diameter.

The equation used to calculate the CNR of the lesions in the breast is as follows:

$$CNR_l = (S_l - S_n) / SD_b$$

where CNR_l = CNR of the lesion in the breast, S_l is the signal intensity of the lesion, S_n is the signal intensity of normal breast tissue, and SD_b is the standard deviation of the noise in the background.

Statistical analysis

The SPSS software package (version 8.0) was used for statistical analysis of the data. Unpaired t-tests were used to compare the mean ADC values, SNR, and CNR between conventional DWI and ASSET-DWI. A *P* value less than 0.05 was considered significant. The mean ADC value of the benign lesions, malignant lesions, and normal breast tissue with different b value also were compared using unpaired t-tests. We used a one side upper limit of 95% permissible interval of ADC was adopted as the point to separate malignant from benign lesions (13): If the ADC value was less than or equal to this threshold, the lesion was considered malignant; if the ADC value was greater than this threshold, the lesion was considered benign. The sensitivity, specificity, and accuracy of ASSET-DWI with different b values were determined.

Results

Comparison of ASSET-DWI and conventional DWI

Image artifacts—Among the 16 lesions in 16 patients studied, three lesions displayed distortion. The ADC values could not be measured in two of three lesions. However, the distortion of normal breast tissue and lesions were reduced by ASSET-DWI, and artifacts resulting from ASSET around the breast did not influence the diagnostic ability of lesion visualization (Figure 1).

SNR and CNR—Because of distortion, the signals of two lesions could not be measured, so the CNR of 14 lesions were analyzed. The SNR of normal breast tissue (n = 7) and the CNR of the lesions (n = 14) obtained using conventional DWI were 9.9 ± 2.04 and 20.38 ± 10.10, respectively, whereas those obtained using ASSET-DWI were 6.17 ± 1.39 and 16.46 ± 9.04, respectively. The SNR of normal breast tissue and the CNR of the lesions obtained with ASSET-DWI were lower compared with those obtained by conventional DWI ($P < 0.05$) (Figure 2).

Mean ADC value—The mean ADC values of the normal breast tissue and breast lesions obtained using conventional DWI were $1.98 \pm 0.30 \times 10^{-3}$ mm^2/s and $1.14 \pm 0.33 \times 10^{-3}$ mm^2/s, respectively, whereas those obtained with ASSET-DWI were $2.03 \pm 0.33 \times 10^{-3}$ mm^2/s and $1.14 \pm 0.33 \times 10^{-3}$ mm^2/s, respectively; these data were not statistically significant ($P > 0.05$).

Lesion detection by ASSET-DWI with different b values

In general, malignant breast lesions exhibited higher signal intensity than benign lesions on ASSET-DWI. In addition, all malignant lesions, except for the two mucinous adenocarcinoma, exhibited a lower signal intensity on the ADC map compared with normal breast tissue. The two mucinous carcinomas showed increased signal intensity on the ADC map relative to normal tissue. All of the benign lesions except for one fibroadenosis displayed increased signal intensity on DWI compared to fatty tissue of the breast (Figure 3, Figure 4).

The mean ADC values of malignant lesions, benign lesions, and normal breast tissue obtained using a b value of 600 s/mm^2 were significantly higher than those obtained using a b value of 1000 s/mm^2 ($P < 0.05$). Using either b value, the mean ADC values of malignant lesions were statistically lower than those of benign lesions and normal breast tissue, and the mean ADC values of benign lesions were significantly lower than those of normal breast tissue ($P < 0.05$) (Table 1).

When b = 600s/mm^2, using the ADC value of 1.44 × 10^{-3} mm^2/s as the diagnostic threshold for a malignant lesion yielded sensitivity of 80% (32/40), specificity of 95% (19/20), and accuracy of 85% (51/60). When b = 1000 s/mm^2 and a threshold ADC value of 1.18×10 $^{-3}$ mm^2/s was used, the sensitivity was 77.5% (31/40), specificity 95% (19/20), and accuracy 83.33% (50/60).

Discussion

The study demonstrated that using ASSET-DWI decreased known EPI distortions and provided excellent differentiation of malignant from benign lesions

The usefulness of DWI has been established in the fields of neuroradiology (8) and in breast (12–17), as mentioned in the introduction. However, traditional EPI-DWI has the disadvantages of susceptibility and phase encoding artifacts, such as chemical shift and ghosting. Parallel imaging techniques such as SENSE and ASSET, are the latest advancements in MR technology, and they enable faster image acquisition time by reducing the number of phase-encoding steps. Our study demonstrated that the use of ASSET combined with DWI could alleviate these problems. By using ASSET-DWI, we were able to obtain images in approximately 50% less time and with decreased EPI distortions compared with conventional EPI-DWI. Presumably, the decrease in image distortion occurred because parallel imaging techniques are capable of reducing the number of phase encoding steps, which leads to reduce phase encode lines and prevents the accumulation of the phase during the single shot read out. Indeed, if full phase encoding steps were use, it would lead to phase accumulation during each phase and severe ghosting.

Our results also demonstrated that the SNR and CNR were decreased with ASSET-DWI compared with conventional DWI. However, by increasing the number of averages, an increase the SNR and the CNR would occur, but at the expense of longer acquisition time. Thus, these factors represent a trade-off between acquisition time and increased SNR need to be considered according to the diagnostic information needed for the study. In addition, with recent hardware advancements, the use of 8 or 16-channel coils, and 3T imaging is becoming more common. The use of more channels and higher field strength will increase SNR and potentially increase the diagnostic ability of breast MR.

Although contrast enhanced MR studies have reported high sensitivity (>90%) (4), breast MR specificity (~85%) for breast cancer needs to be improved (5). Our results illustrate that the ADC map value obtained by ASSET-DWI can differentiate malignant from benign lesion of the breast and may help to increase specificity. We found that using a b value of either 0, 600s/mm^2 or 0, 1000s/mm^2, the mean ADC values of malignant lesions were in general lower than those of benign lesions and normal breast tissue, which is consistent with previously published results (13–17). The decreased ADC values in malignant lesions could potentially help in differentiating benign and malignant breast tumors. The reasons why malignant tumors have lower ADC values are poorly understood but is probably related to a combination of higher cellularity, tissue disorganization, and increased extracellular space tortuosity, all contributing to reduced motion of water. Correlations with cellularity have been found for some neoplasms including breast lesions but not for all tumors (19–23). Histological examinations have shown increased cellularity of malignant breast tumors compared to benign lesions (24). Hatakenaka et al. reported an inverse correlation between ADC and tumor cellularity (23).

Our results also revealed overlap still existed between benign and malignant lesions. In our study, as for a false negative case, the mucinous carcinoma showed very high ADC values, the low density of tumor cells and a large amount of mucus around the tumor cells which reflected a ‘mucoid lake’ were observed in the pathologic image (Figure 5). Possibly, the

relatively decreased cellularity in the tumors increases the diffusion speed of water molecules in the extracellular fluid. As for a false positive case, the intraductal papilloma showed relatively low ADC value, the high cell density with small extracellular space was found in this case. Woodhams et al (25) also reported that most intraductal papilloma had low ADC values. Besides, some invasive ductal carcinomas demonstrated relatively high ADC values, and if the ADC values were higher than the diagnostic threshold for a malignant lesion, these will induced the false negative cases.

The b value and the diagnostic threshold of the ADC value in ASSET-DWI

In biologic tissues, microscopic motion includes both the molecular diffusion of water and the blood microcirculation in the capillary network, and both diffusion and perfusion effects can influence the ADC map values. DWI is obtained by acquiring T2-weighted images with the addition of diffusion weighting gradient around the refocusing pulse using a combination of timing events, known as the “b value”. On DWI obtained with a low b-value, perfusion effects usually cause larger signal attenuation than diffusion effects (26,27). At a high b value, ADC measurement will be relatively perfusion insensitive and ADC map value is close to the true diffusion coefficient *D* (28,29). Therefore, high b values are recommended for breast DWI (b > 500). But the optimal b value has not been established and there is no general census. To date, several studies have reported the ADC map values of malignant and benign breast lesions using a variety of b values ranging from 400 s/mm^2 to 1000 s/mm^2 (14–17), for example, mean ADC map values of malignant lesions reported by Sinha et al. (14): $1.60 \pm 0.36 \times 10^{-3}$ mm^2/s (b = 400); Kinoshita et al. (15): $1.22 \pm 0.19 \times 10^{-3}$ mm^2/s (b = 700); Woodhams et al. (16), $1.12 \pm 0.24 \times 10^{-3}$ mm^2/s (b = 750); Guo et al. (13): $0.97 \pm 0.20 \times 10^{-3}$ mm^2/s (b = 1,000) and Park et al. (17): $0.89 \pm 0.18 \times 10^{-3}$ mm^2/s (b = 1000). Park et al suggested high b values (1000 s/mm^2) could obtain diffusion information without significant image distortion. In addition, they have suggested that the ADC map value of breast lesions should be compared to normal fibroglandular tissue because of potential variability in the ADC map value due to gradient factors (17). Thus, the optional b value is still under investigation. In our study, we compared the ADC values between b value of 0, 600 s/mm^2 and 0, 1000 s/mm^2. Our results confirmed that the mean ADC map values of malignant lesions, benign lesions, and normal breast tissue were all lower at b = 1000 s/mm^2 than at b = 600 s/mm^2. In addition, the diagnostic sensitivity and specificity were not increased at the higher b value compared to the lower b value. Based on our results, we found a diagnostic threshold of ADC map values based on b values of 600 s/mm^2 or 1000 s/mm^2.

Limitations of the study

Our study has some limitations. First, in this study, we used 4-mm slice thickness to ensure there was sufficient SNR for lesion detection. If the lesion in the breast is smaller than 4-mm in diameter, the ADC map value perhaps can not be measured exactly because of the partial volume effect. Therefore, DWI should be performed in conjunction with contrast-enhanced MRI. Second, because the ADC map value varies according to b value, our study suggested that the diagnostic ADC value threshold for malignant tumors and the b value used in breast DWI should be standardized through large studies conducted at multiple medical centers. Finaly, overlap still exists between benign and malignant lesions as revealed in our results. Therefore, ADC map values maybe unreliable for mucinous carcinoma and intraductal papilloma.

Conclusions

ASSET-DWI can be used to evaluate breast tissue with decreased distortion, susceptibility to artifacts, and acquisition time compared to other methods. The use of DWI is feasible and

offers increased specificity with b values ranging from 600 to 1000 s/mm^2. ADC map values of breast lesions can be used to further characterize malignant lesions from benign ones.

Acknowledgments

This work was supported in part by NIH 1R01CA100184

References

1. Heywang SH, Fenzl G, Beck R, et al. Use of Gd-DTPA in the nuclear magnetic resonance study of the breast. Rofo 1986;145:565–571. [PubMed: 3024255]
2. Kaiser WA, Zeitler E. MR imaging of the breast: fast imaging sequences with and without Gd-DTPA. Preliminary observations. Radiology 1989;170:681–686. [PubMed: 2916021]
3. Kuhl CK, Mielcareck P, Klaschik S, et al. Dynamic breast MR imaging: are signal intensity time course data useful for differential diagnosis of enhancing lesions? Radiology 1999;211:101–110. [PubMed: 10189459]
4. Lehman CD, Schnall MD. Imaging in breast cancer: magnetic resonance imaging. Breast Cancer Res 2005;7:215–219. [PubMed: 16168141]
5. Bluemke DA, Gatsonis CA, Chen MH, et al. Magnetic resonance imaging of the breast prior to biopsy. JAMA 2004;292:2735–2742. [PubMed: 15585733]
6. Choi N, Han BK, Choe YH, et al. Three-phase dynamic breast magnetic resonance imaging with two-way subtraction. J Comput Assist Tomogr 2005;29:834–841. [PubMed: 16272861]
7. Le Bihan D, Breton E, Lallemand D, et al. MR imaging of intravoxel incoherent motions: application to diffusion and perfusion in neurologic disorders. Radiology 1986;161:401–407. [PubMed: 3763909]
8. Barber PA, Hill MD, Eliasziw M, et al. Imaging of the brain in acute ischaemic stroke: comparison of computed tomography and magnetic resonance diffusion-weighted imaging. J Neurol Psychiatry 2005;76:1528–1533.
9. Chenevert TL, Stegman LD, Taylor JM, et al. Diffusion magnetic resonance imaging: an early surrogate marker of therapeutic efficacy in brain tumors. J Natl Cancer Inst 2000;92:2029–2036. [PubMed: 11121466]
10. Kucharczyk J, Mintorovitch J, Asgari HS, et al. Diffusion/perfusion MR imaging of acute cerebral ischemia. Magn Reson Med 1991;19:311–315. [PubMed: 1881320]
11. Brunberg JA, Chenevert TL, McKeever PE, et al. In vivo MR determination of water diffusion coefficients and diffusion anisotropy: correlation with structural alteration in gliomas of the cerebral hemispheres. AJNR Am J Neuroradiol 1995;16:361–371. [PubMed: 7726086]
12. Englander SA, Uluğ AM, Brem R, et al. Diffusion imaging of human breast. NMR Biomed 1997;10:348–352. [PubMed: 9471126]
13. Guo Y, Cai YQ, Cai ZL, et al. Differentiation of clinically benign and malignant breast lesions using diffusion-weighted imaging. J Magn Reason Imaging 2002;16:172–178.
14. Sinha S, Lucas-Quesada FA, Sinha U, et al. In vivo diffusion-weighted MRI of the breast: potential for lesion characterization. J Magn Reson Imaging 2002;15:693–704. [PubMed: 12112520]
15. Kinoshita T, Yashiro N, Ihara N, et al. Diffusion-weighted half-Fourier single-shot turbo spin echo imaging in breast tumor: differentiation of invasive ductal carcinoma from fibroadenoma. J Comput Assist Tomogr 2002;26:1042–1046. [PubMed: 12488758]
16. Woodhams R, Matsunaga K, Iwabuchi K, et al. Diffusion-weighted imaging of malignant breast tumors: the usefulness of apparent diffusion coefficient (ADC) value and ADC map for the detection of malignant breast tumors and evaluation of cancer extension. J Comput Assist Tomogr 2005;29:644–649. [PubMed: 16163035]
17. Park MJ, Cha ES, Kang BJ, et al. The role of diffusion-weighted imaging and the apparent diffusion coefficient (ADC) values for breast tumors. Korean J Radiol 2007;8:390–396. [PubMed: 17923781]

18. Kuroki Y, Nas K, Kuroki S, et al. Diffusion-weighted imaging of breast cancer with the sensitivity encoding technique: analysis of the apparent diffusion coefficient value. Magn Reson Med Sci 2004;3:79–85. [PubMed: 16093623]

19. Humphries PD, Sebire NJ, Siegel MJ, et al. Tumors in pediatric patients at diffusion-weighted MR imaging: apparent diffusion coefficient and tumor cellularity. Radiology 2007;245(3):848–854. [PubMed: 17951348]

20. Squillaci E, Manenti G, Cova M, et al. Correlation of diffusion-weighted MR imaging with cellularity of renal tumours. Anticancer Res 2004;24(6):4175–4179. [PubMed: 15736469]

21. Manenti G, Di Roma M, Mancino S, et al. Malignant renal neoplasms: correlation between ADC values and cellularity in diffusion weighted magnetic resonance imaging at 3 T. Radiol Med 2008;113(2):199–213. [PubMed: 18386122]

22. Sugahara T, Korogi Y, Kochi M, et al. Usefulness of diffusion-weighted MRI with echo-planar technique in the evaluation of cellularity in gliomas. J Magn Reson Imaging 1999;9:53–60. [PubMed: 10030650]

23. Hatakenaka M, Soeda H, Yabuuchi H, et al. Apparent diffusion coefficients of breast tumors: clinical application. Magn Reson Med Sci 2008;7:23–29. [PubMed: 18460845]

24. Ducatman BS, Emery ST, Wang HH. Correlation of histologic grade of breast carcinoma with cytologic features on fine-needle aspiration of the breast. Mod Pathol 1993;6:539–543. [PubMed: 8248109]

25. Woodhams R, Matsunaga K, Kan S, et al. ADC mapping of benign and malignant breast tumors. Magn Reson Med Sci 2005;4:35–42. [PubMed: 16127252]

26. Le Bihan D, Breton E, Lallemand D, et al. Separation of diffusion and perfusion in intravoxel incoherent motion MR imaging. Radiology 1988;168:497–505. [PubMed: 3393671]

27. Morvan D. In vivo measurement of diffusion and pseudo-diffusion in skeletal muscle at rest and after exercise. Magn Reson Imaging 1995;13:193–199. [PubMed: 7739360]

28. Thoeny HC, De Keyzer F, Boesch C, et al. Diffusion-weighted imaging of the parotid gland: Influence of the choice of b-values on the apparent diffusion coefficient value. J Magn Reson Imaging 2004;20:786–790. [PubMed: 15503336]

29. Wheeler-Kingshott CA, Thomas DL, Lythgoe MF, et al. Burst excitation for quantitative diffusion imaging with multiple b-values. Magn Reson Med 2000;44:737–745. [PubMed: 11064409]

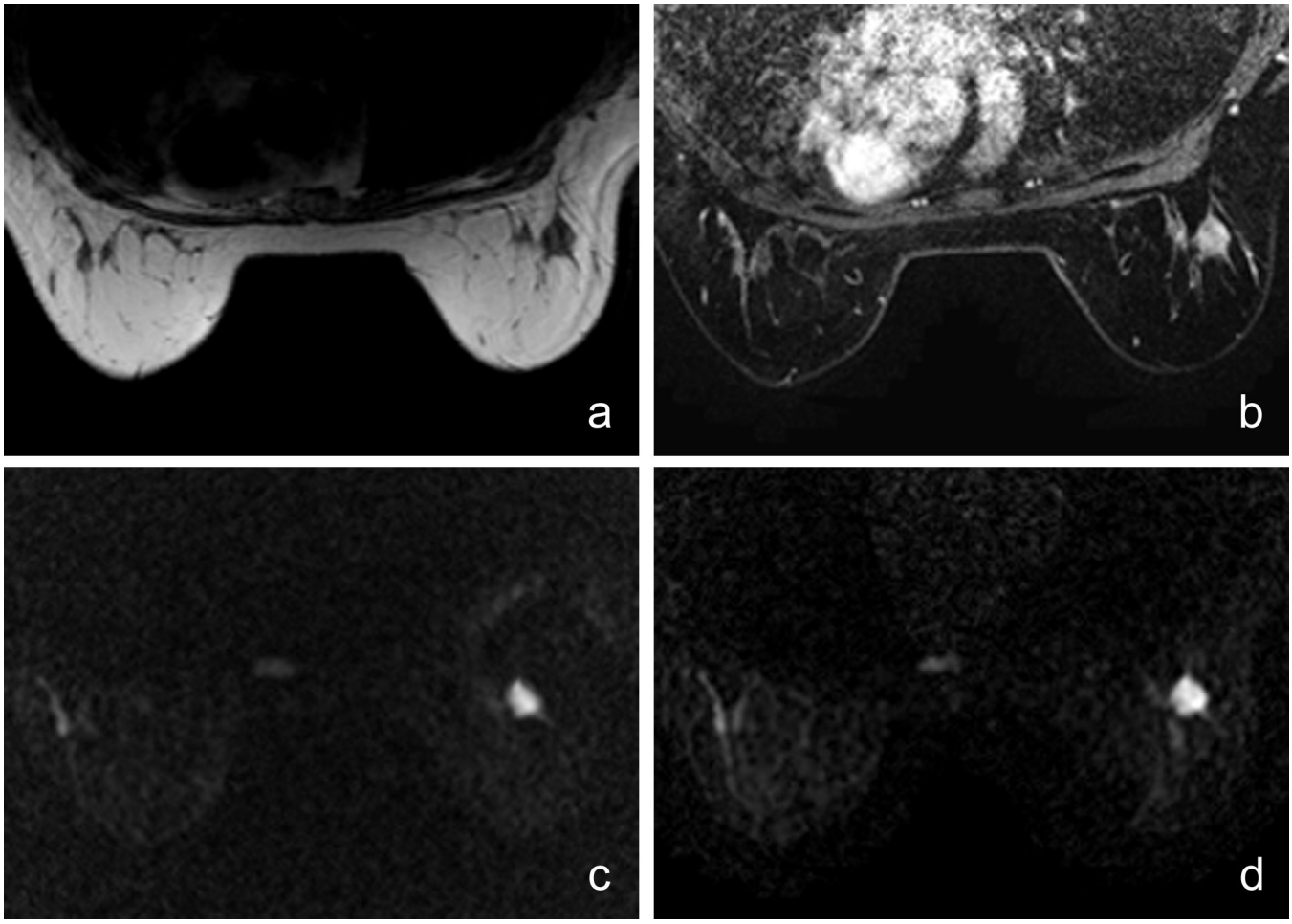

Fig. 1.

A 43-year-old woman with invasive ductal carcinoma in the right breast. (a) The SE T1WI axial scan showed a slightly hypointense lesion in the right breast. (b) Dynamic contrast magnetic resonance imaging revealed the enhaned lesion. The lesion showed distortion on traditional DWI (b = 0, 1000 s/mm^2) (c) compared with SE T1WI (a) on the same slice, but the distortion was decreased with ASSET-DWI (b = 0, 1000 s/mm^2) (d).

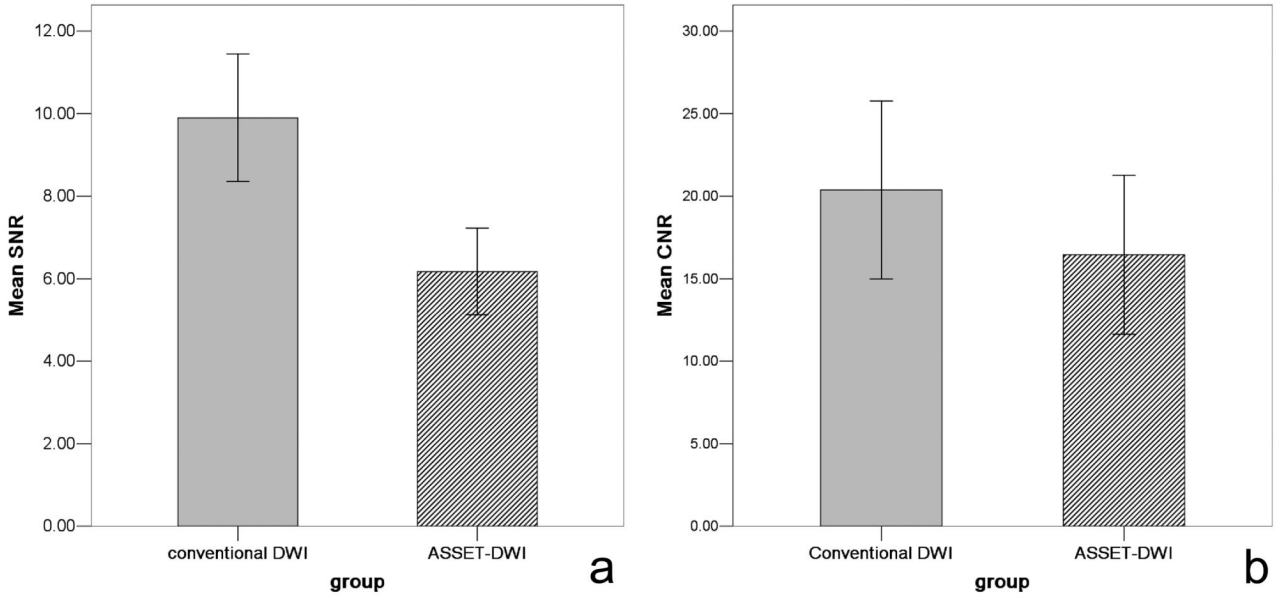

Fig. 2.
The comparison of SNR (a) and CNR (b) between the conventional DWI and ASSET-DWI.

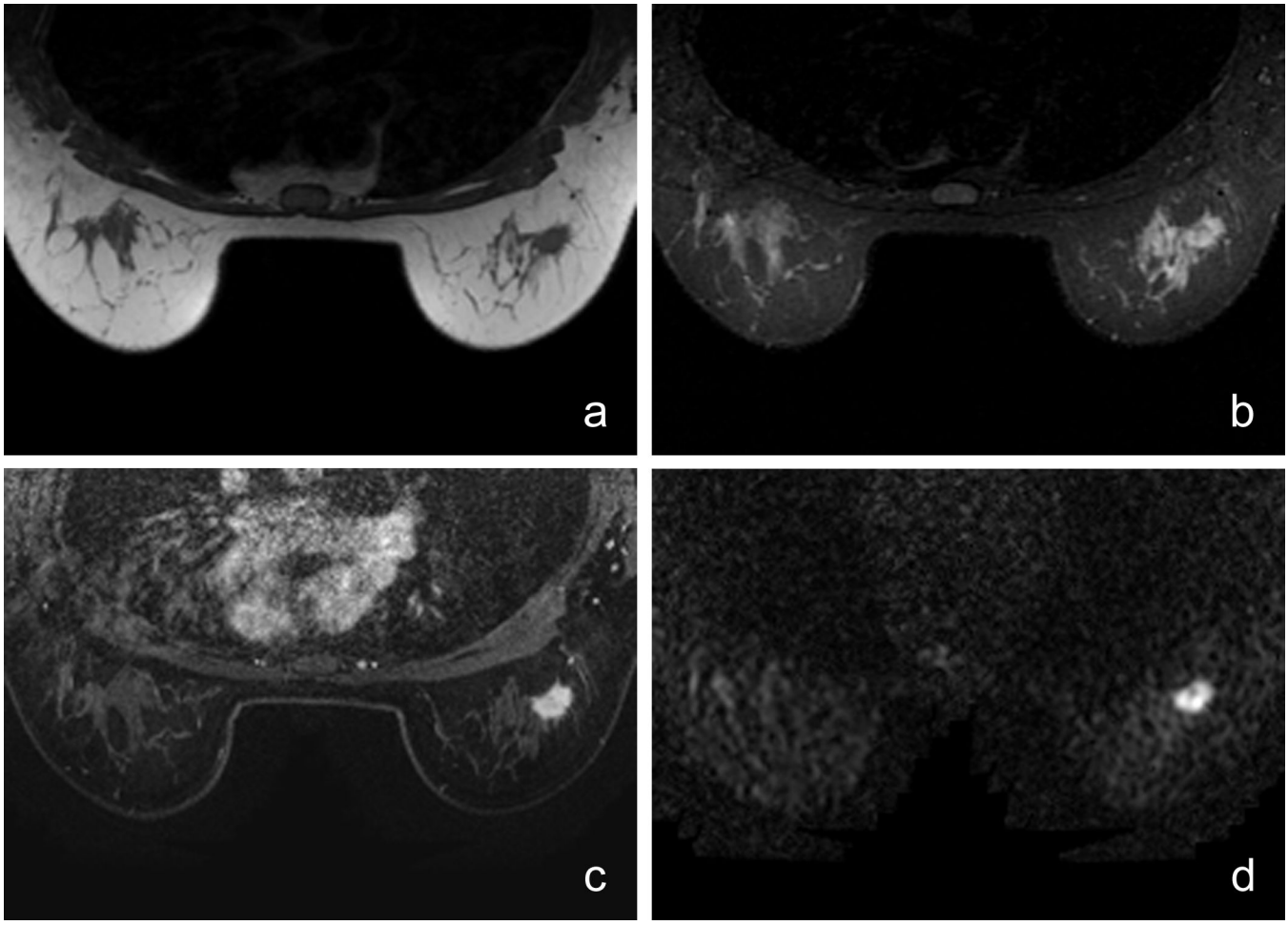

Fig.3.

A 29-year-old woman with invasive ductal carcinoma in the right breast. (a) A mass found in the right breast was hypointense on the axial SE T1WI. (b) The lesion exhibited a slightly high signal intensity on axial T2WI STIR. (C) The lesion was obviously enhanced but with an ill-defined margin on the dynamic contrast image. (d) The lesion showed high signal intensity on ASSET-DWI (b = 1000 s/mm^2).

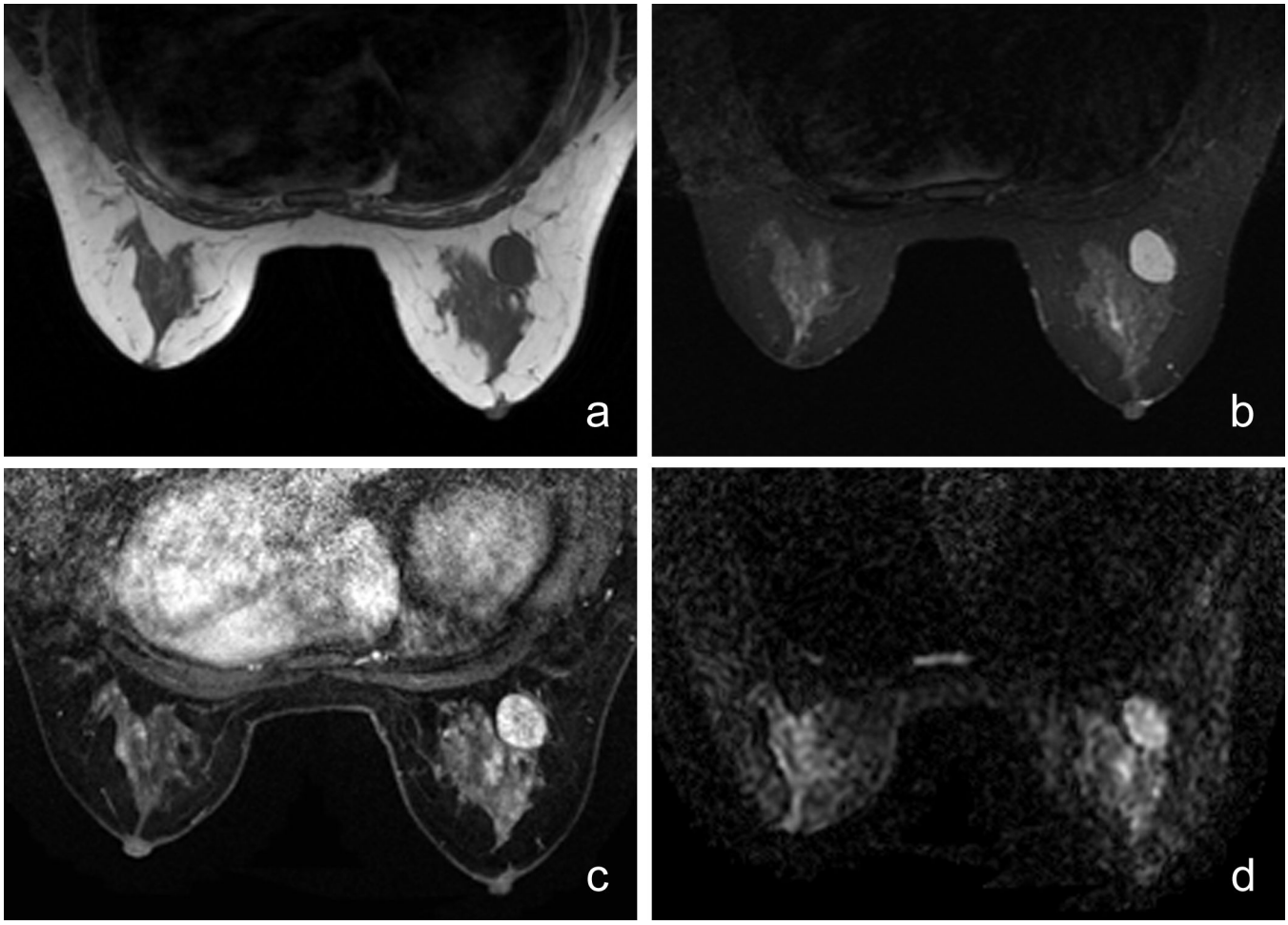

Fig.4.

A 53-year-old woman with fibroadenoma in the right breast. (a) A mass found in the right breast was hypointense on the axial SE T1-WI. (b) The lesion showed high signal intensity on axial T2WI STIR. (C) The lesion was enhanced with a well-defined margin on the dynamic contrast image. (d) The lesion showed slightly high signal on ASSET-DWI (b = 1000 s/mm^2).

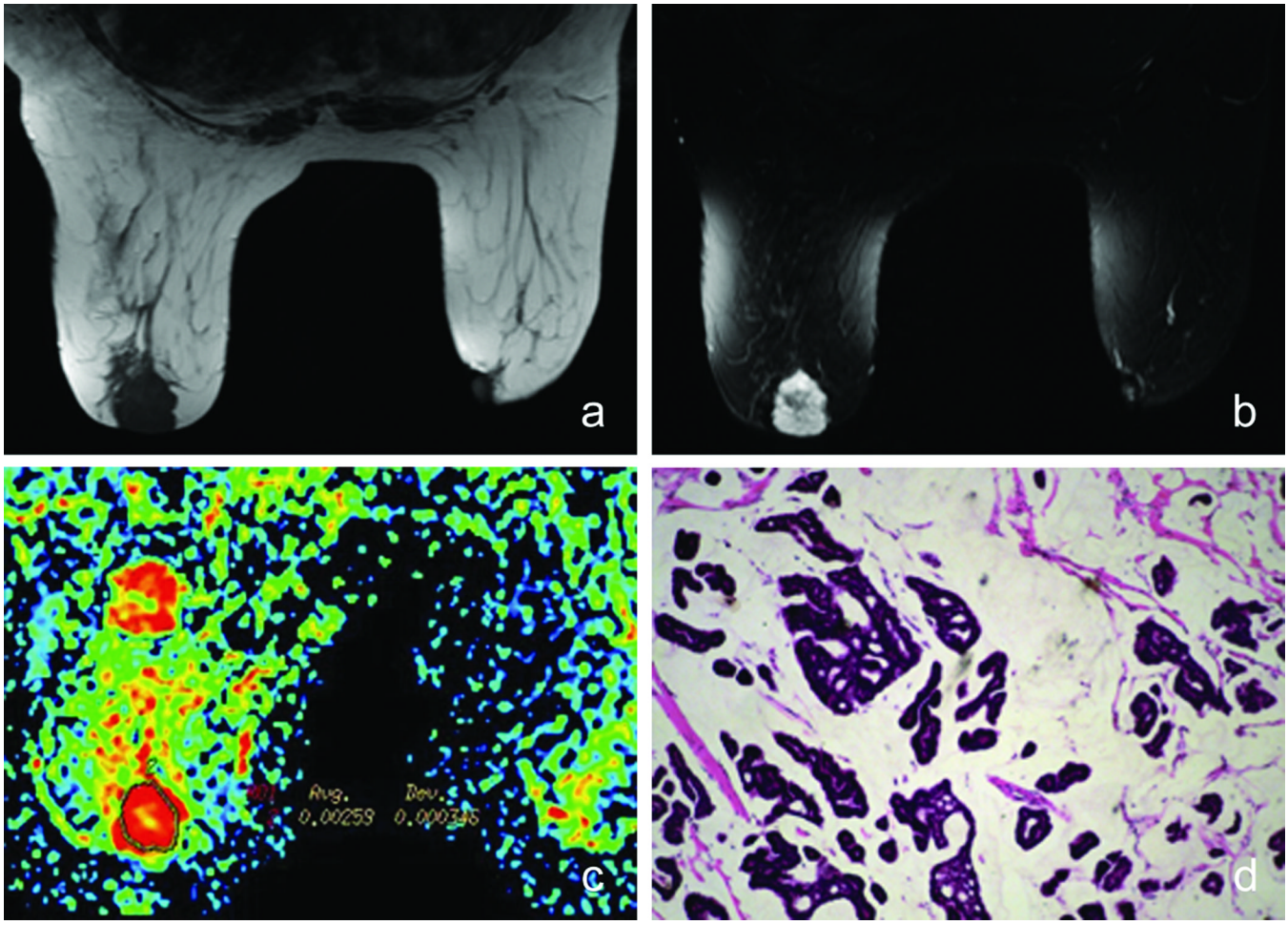

Fig. 5.

An 80-year-old woman with mucinous adenocarcinoma in the left breast. (a) A mass found in the left breast showed low signal intensity on the axial SE T1WI. (b) The lesion showed high signal intensity on axial T2WI STIR. (c) The ADC color map showed that the ADC map value of the lesion was 2.59×10^{-3} mm^2/s ($b = 1000$ s/mm^2). (d) The pathological image of the tumor after resection (HE staining × 40). The low density of tumor cells and a large amount of mucus around the tumor cells which reflected a ‘mucoid lake’ were observed.

Table 1

The mean ADC values of benign lesions, malignant lesions, and normal breast tissue obtained using different b values

Group	N	Mean ADC value ($\times 10^{-3}$ mm^2/s)	Range of 95% confidence ($\times 10^{-3}$ mm^2/s)
b = 600s/mm^2			
Malignant	40	1.33 ± 0.36$^{*\#}$	1.21–1.44
Benign	20	1.82 ± 0.31^{+}	1.68–1.97
Normal	20	2.05 ± 0.33	1.90–2.21
b = 1000s/mm^2			
Malignant	40	1.08 ± 0.32$^{*\#}$	0.97–1.18
Benign	20	1.61 ± 0.33^{+}	1.45–1.76
Normal	20	1.85 ± 0.33	1.70–2.0

$^{*}P < 0.05$ indicates comparison between malignant and benign lesions,

$^{\#}P < 0.05$ between malignant lesions and normal breast tissue, and

$^{+}P < 0.05$ between benign lesions and normal breast tissue.